Optical and Quantum Electronics **10** *(1978) 31–40*

Propagation in radially-inhomogeneous single-mode fibre

W. A. GAMBLING, H. MATSUMURA
Department of Electronics, University of Southampton, Southampton SO9 5NH, UK

Received 29 June 1977; revised 12 September 1977

The propagation of electromagnetic waves along a radially-inhomogeneous single-mode optical fibre with small index difference between core and cladding is studied. As in the case of the step-index fibre the propagation modes are weakly guided and their transverse fields are essentially polarized in one direction. The simple field descriptions and characteristic equation obtained here enable mode spot size and bending loss to be determined and are useful for practical design work of radially-inhomogeneous single-mode optical fibres.

1. Introduction

A refractive-index profile having a carefully chosen distribution [1] is normally introduced into multimode fibres in order to maximize the available bandwidth. The WKB method may be used for the analysis of such multimode graded-index fibres [1] but is not suitable for single-mode fibres. Studies of single-mode fibres tend to assume a stepped refractive-index distribution but in practice even a small amount of diffusion at the core/cladding interface during fabrication [2] may produce an appreciable profiling effect [3] due to the small core size. It is important to determine the effect such profiling has on the fibre characteristics.

Single-mode fibres can be analysed by direct solution of the wave equation [4], by a power-series expansion [5] and by variational techniques [6, 7] with varying degrees of accuracy. Unfortunately all these methods are rather tedious and involve considerable effort to deduce the field equations, characteristic equation, etc. We therefore calculate the field equations for a radially-inhomogeneous single-mode fibre by a simplified method making only the assumption

$$\Delta \ll 1 \tag{1}$$

where Δ is the relative refractive index difference between that at the centre of the core (n_1) and in the cladding (n_2) i.e.

$$\Delta = \frac{(n_1^2 - n_2^2)}{2n_1^2} \simeq \frac{n_1 - n_2}{n_1}.$$

In a step-index, single-mode fibre the modes that propagate under the above condition are weakly guided and are essentially polarized linearly [8]. We show that the same is true for a radially-inhomogeneous fibre and from the field equations we deduce the spot size of the HE_{11} mode and the bending loss.

2. Field distribution and characteristic equation

Consider a cylindrical fibre in which the dielectric constant varies only in the transverse (radial) direction r as

$$\begin{aligned} \epsilon(R) &= \epsilon_1(1 - 2\Delta R^{\alpha}) \qquad \text{for } 0 \leqslant R \leqslant 1 \\ &= \epsilon_1(1 - 2\Delta) = \epsilon_2 \qquad \text{for } R \geqslant 1 \end{aligned} \tag{2}$$

where $R = r/a$ = normalized fibre radius, a = core radius and α = parameter between 1 and ∞ which describes the index profile in the fibre core.

As indicated above we assume $\Delta \ll 1$.

Solutions are sought in cylindrical coordinates (r, θ, z) for the electric and magnetic field components of the type:

$$\begin{aligned} E_r &= e_r(R)S_2(\theta, z) \\ E_\theta &= e_\theta(R)S_1(\theta, z) \\ E_z &= j(2\Delta/V^2)^{1/2}e_z(R)S_2(\theta, z) \end{aligned} \tag{3}$$

and

$$\begin{aligned} H_r &= h_r(R)S_1(\theta, z) \\ H_\theta &= h_\theta(R)S_2(\theta, z) \\ H_z &= j(2\Delta\epsilon'/\mu V^2)^{1/2}h_z(R)S_1(\theta, z) \end{aligned} \tag{4}$$

where

$$S_1(\theta, z) = \begin{Bmatrix} \sin(n\theta) \\ \text{or} \\ \cos(n\theta) \end{Bmatrix} \exp(-j\beta z) \quad S_2(\theta, z) = \begin{Bmatrix} \cos(n\theta) \\ \text{or} \\ -\sin(n\theta) \end{Bmatrix} \exp(-j\beta z); \tag{5}$$

and

$$\epsilon' = \begin{cases} \epsilon_1 & \text{for } 0 \leqslant R \leqslant 1 \\ \epsilon_2 & \text{for } 1 \leqslant R. \end{cases} \tag{6}$$

V is the normalized frequency defined by

$$V^2 = 2\omega^2\mu\epsilon_1 a^2\Delta. \tag{7}$$

By using the method of Kurtz and Streifer [4] the electric and magnetic fields in the core can be expressed as

$$\begin{aligned} e_r(R) &= A_1\phi_1 + A_2\phi_2 \\ e_\theta(R) &= -A_1\phi_1 + A_2\phi_2 \\ e_z(R) &= A_1G_1 + A_2G_2 \\ h_r(R) &= (\epsilon_1/\mu)^{1/2}(A_1\phi_1 - A_2\phi_2) \\ h_\theta(R) &= (\epsilon_1/\mu)^{1/2}(A_1\phi_1 + A_2\phi_2) \\ h_z(R) &= A_1G_1 - A_2G_2 \end{aligned} \tag{8}$$

where functions ϕ_i and G_i $(i = 1, 2)$ satisfy

$$\frac{d^2\phi_i}{dR^2} + \frac{1}{R}\frac{d\phi_i}{dR} + \left[U^2 - V^2R - \frac{(n \mp 1)^2}{R^2}\right]\phi_i = 0 \tag{9}$$

and

$$G_i = -\frac{d\phi_i}{dR} - \frac{(1 \mp n)}{R}\phi_i. \tag{10}$$

The upper (lower) sign corresponds to $i = 1$ (2) and A_1 and A_2 are constants. The parameter U in the core is defined as

$$U^2 = \omega^2\mu\epsilon_1 a^2 - \beta^2 a^2. \tag{11}$$

The field in the cladding can be obtained in a similar way. The parameter W in this case can be defined as

$$W^2 = \beta^2 a^2 - \omega^2\mu\epsilon_2 a^2 \tag{12}$$

so that

$$V^2 = U^2 + W^2. \tag{13}$$

The electric and magnetic field components in the cladding are given in terms of the modified Hankel function by:

$$
\begin{aligned}
e_r(R) &= \left[\frac{n}{R}(C-D)K_n(WR) + CWK_{n-1}(WR)\right]W^{-2} \\
e_\theta(R) &= \left[\frac{n}{R}(C-D)\,K_n(WR) - DWK_{n-1}(WR)\right]W^{-2} \\
e_z(R) &= CK_n(WR) \\
h_r(R) &= -(\epsilon_2/\mu)^{1/2}e_\theta(R) \\
h_\theta(R) &= (\epsilon_2/\mu)^{1/2}e_r(R) \\
h_z(R) &= DK_n(WR)
\end{aligned}
\tag{14}
$$

C and D are constants.

The continuity of E_z, H_z, E_θ and H_θ at the boundary ($R = 1$) provides the unknown constants and the eigenvalue equation. Thus

$$
\left[\frac{K_{n+1}(W)}{WK_n(W)}g_2 - \phi_2\right]\left[\frac{K_{n-1}(W)}{WK_n(W)}g_1 - \eta\phi_1\right] + \left[\frac{K_{n+1}(W)}{WK_n(W)}g_2 - \eta\phi_2\right]\left[\frac{K_{n-1}(W)}{WK_n(W)}g_2 - \phi_1\right] = 0 \tag{15}
$$

and

$$
C = \frac{A_1g_1 + A_2g_2}{K_n(W)} \qquad D = \frac{A_1g_1 - A_2g_2}{K_n(W)} \tag{16}
$$

$$
A_1\left[\frac{K_{n-1}(W)}{WK_n(W)}g_1 - \phi_1\right] = A_2\left[\frac{K_{n+1}(W)}{WK_n(W)}g_2 - \phi_2\right].
$$

Here, g_i and ψ_i are values of G_i and ϕ_i at $R = 1$, respectively, and $\eta = (\epsilon_1/\epsilon_2)^{1/2}$. As $\eta \to 1$ then the eigenvalue equation (Equation 15) decomposes into the two characteristic equations

$$
\begin{aligned}
\frac{g_1}{\psi_1} &= \frac{WK_n(W)}{K_{n-1}(W)} \quad \text{representing } HE_{nm} \text{ modes} \\
\frac{g_2}{\psi_2} &= \frac{WK_n(W)}{K_{n+1}(W)} \quad \text{representing } EH_{nm} \text{ modes.}
\end{aligned}
\tag{17}
$$

Substitution of Equation 17 into Equation 16 gives $A_2 = 0$ for HE_{nm} modes and $A_1 = 0$ for EH_{nm} modes. The field equations and characteristic equations for the TE_{0m} and TM_{0m} modes are obtained simply by setting $n = 0$.

Equations 9, 10 and 17 show that the HE_{nm} and $EH_{n-2,m}$ modes ($n > 2$), and the HE_{2m} and TE_{0m} (or TM_{0m}) modes are identical. When $\eta \neq 1$, this degeneracy ceases to exist, but in most practical cases the approximation $\eta = 1$ gives good results. This degeneracy results in linearly polarized LP_{lm} modes [6], the properties of which may be deduced from the field equations, 8 and 14. Thus the field components of the LP_{lm} modes polarized in the y direction are

$$
E_y = A\phi_l(R)\begin{bmatrix}\sin(l\theta)\\ \text{or}\\ \cos(l\theta)\end{bmatrix}
$$

$$
H_x = -A(\epsilon_1/\mu)^{1/2}\phi_l(R)\begin{bmatrix}\sin(l\theta)\\ \text{or}\\ \cos(l\theta)\end{bmatrix}
$$

$$
E_z = j(2\Delta/V^2)^{1/2}A\left\{H_{1l}(R)\begin{bmatrix}\cos(l-1)\theta\\ \text{or}\\ -\sin(l-1)\theta\end{bmatrix} - H_{2l}(R)\begin{bmatrix}\cos(l+1)\theta\\ \text{or}\\ -\sin(l+1)\theta\end{bmatrix}\right\}
$$

$$H_z = -j(2\Delta\epsilon_1/\mu V^2)^{1/2}A\left\{H_{1l}(R)\begin{bmatrix}\sin(l-1)\theta\\ \text{or}\\ \cos(l-1)\theta\end{bmatrix} + H_{2l}(R)\begin{bmatrix}\sin(l+1)\theta\\ \text{or}\\ \cos(l+1)\theta\end{bmatrix}\right\} \tag{18}$$

where

$$\phi_l(R) = P_l(R) \qquad \text{in the core}$$

$$= P_l(R=1)\frac{K_l(WR)}{K_l(W)} \qquad \text{in the cladding}$$

and

$$H_{il} = -\frac{\mathrm{d}\phi_l(R)}{\mathrm{d}R} + (-1)^i\frac{l}{R}\phi_l(R) \quad \text{for } i = 1, 2. \tag{19}$$

Function $P_l(R)$ is obtained from the differential equation

$$\frac{\mathrm{d}^2P_l}{\mathrm{d}R^2} + \frac{1}{R}\cdot\frac{\mathrm{d}P_l}{\mathrm{d}R} + [U^2 - V^2R^\alpha - l^2/R^2]P_l = 0. \tag{20}$$

The characteristic equation of the LP_{lm} modes is given by

$$\frac{WK_{l+1}(W)}{K_l(W)} = \left.\frac{-\mathrm{d}P_l(R)/\mathrm{d}R}{P_l(R)}\right|_{R=1} + l. \tag{21}$$

3. Propagation characteristics of a single-mode fibre

The propagation characteristics of a single-mode, graded-index fibre can be evaluated by setting $l = 0$. For this particular case the second-order differential equation (Equation 20) can be easily solved by the series expansion method, since the series converges rapidly due to the small V, U values. (In multimode fibres Equation 20 can be solved by the WKB method.) Thus a series solution is assumed, in the interval $0 \leqslant R < 1$, of the form

$$P_0(R) = \sum_{q=0}^{\infty} a_q R^q. \tag{22}$$

Substitution into Equation 20 and equating coefficients of each power of R produces a set of equations in the coefficients a_q as follows:

$$\begin{aligned}
a_0 &= 1\\
a_1 &= 0\\
a_2 &= -a_0U^2/2^2\\
&\vdots\\
a_{\alpha+1} &= -a_{\alpha-1}U^2/(\alpha+1)^2\\
a_{\alpha+2} &= -(a_\alpha U^2 - a_0V^2)/(\alpha+2)^2\\
a_{\alpha+3} &= -(a_{\alpha+1}U^2 - a_1V^2)/(\alpha+3)^2\\
&\vdots
\end{aligned} \tag{23}$$

When α is large enough the coefficients a_q become Bessel functions of zero order, as would be expected for a step-index fibre ($\alpha = \infty$). For any other value of α, all the relevant parameters (V, U, W and β) can be obtained from the characteristic equation (Equation 21) for $l = 0$. For example Fig. 1 shows the U–V curves of the HE_{11} mode for various values of α from which the propagation constant β can be obtained since $\beta a = (V^2/2\Delta - U^2)^{1/2}$. It may be seen that for a given normalized frequency V the value of U increases as α decreases, i.e. with departure from a step-index profile. However little change occurs as α falls from ∞ to 50 while an α of 14 is necessary before U increases by 5%. Thereafter the

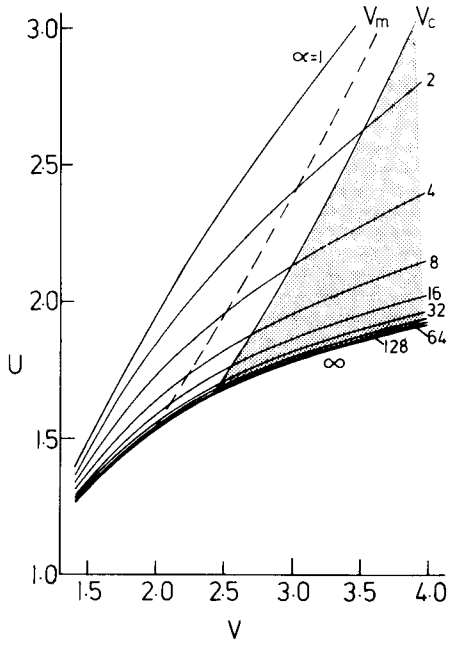

Figure 1 Variation of U with normalised frequency for the HE_{11} mode in fibres of various refractive-index profiles. The speckled area denotes the region of multimode operation. The dashed line indicates the conditions for which the spot size is a minimum.

effect of optical smoothing of the profile becomes more evident and, for example, at $V = 2.5$ a parabolic profile changes U to 2.14 compared with 1.67 for a step-index. For the particular case of a parabolic profile it is possible to make a comparison with the results of Dil and Blok [5]. For $\alpha = 2$ there is good agreement (within a few percent) with their Fig. 3 thus justifying the use of the approximations made here.

Comparison with the results given in [3] shows good agreement with the cut-off value of the LP_{11} mode calculated from Equations 20 and 21. It can be seen that, as with U, changes in α from that corresponding to a step-index profile down to ~ 50 has little effect on V_c. Thereafter the change is more rapid and for a parabolic profile V_c has increased to 3.518. The use of a graded profile in single-mode fibres may thus reduce the restrictions on core diameter and ease to some extent the problems of jointing, launching and coupling.

The normalized intensity distributions of the HE_{11} mode for various α are shown in Fig. 2 for both single-mode (a) and multimode (b) conditions. In both cases the field intensity falls off more rapidly at lower values of α as might be expected from the reduced degree of guidance in the core.

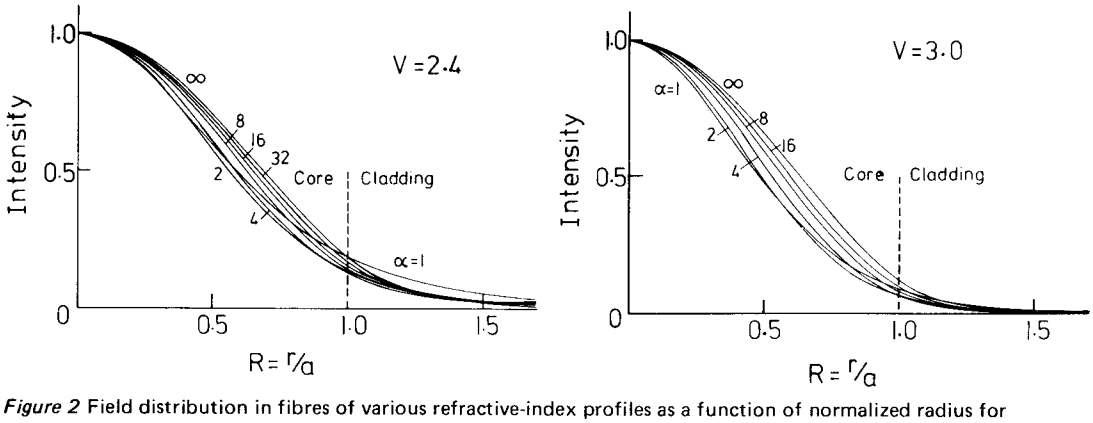

Figure 2 Field distribution in fibres of various refractive-index profiles as a function of normalized radius for (a) $V = 2.4$, (b) $V = 3.0$.

4. Spot size of HE_{11} mode in radially-inhomogeneous fibre

An important feature of propagation in single-mode fibres is the loss due to microbending. Petermann [9] has reported that by restricting the index difference and normalized frequency in a single-mode fibre the microbending loss can be made small since it increases appreciably with spot size of the HE_{11} mode which in turn is a function of V. The spot size of the HE_{11} mode is defined by Petermann as:

$$w_0^2 = \int_0^\infty r^3 E_y^2 \, dr \Big/ \int_0^\infty r E_y^2 \, dr. \tag{24}$$

However we propose a different and simpler definition [10] which is first explained by reference to a step-index fibre. We then show that the spot size given by Equation 24 is in good agreement with our definition.

The excitation efficiency of the HE_{11} mode by a Gaussian beam varies with the normalized frequency of a fibre. In the region well above cut-off [11] the maximum excitation efficiency (about 97%) can be obtained with a Gaussian beam having a spot size (to $1/e$ intensity) of about $0.48a$. For the single-mode region [12], the maximum excitation efficiency and the corresponding normalized spot size of the input beam are shown in Fig. 3 as a function of V. The excitation efficiency exceeds 99% for normalized frequencies between 2.0 and the cut-off value 2.4 because the field distribution of the HE_{11} mode is then very similar to that of a Gaussian beam. Therefore we define the spot size of the HE_{11} mode as that of the input TEM_{00} laser beam at which the maximum excitation efficiency is obtained. This is a transformation of the definition from the field distribution of the HE_{11} mode inside the fibre, expressed in terms of Equation 24, to the external Gaussian distribution producing the best match. Fig. 4 compares the definitions as a function of V for a step-index fibre; the dashed curve is obtained from Equation 24 and the solid one is from our new definition (Fig. 3). The divergence of the two curves for small V is due to the lower excitation efficiency. Nevertheless the two methods are in good agreement (within 1% at $V = 2.4$) particularly at the V values of most interest. It should be noted that these definitions of spot size differ from the 1/e intensity width of the HE_{11} mode in the core.

Using this new definition which we have shown to be valid for the step-index fibre we have calculated the normalized spot size of graded fibres from that of the input Gaussian beam which gives maximum launching efficiency. It can be seen from Fig. 5 that the normalized spot size varies with α and in general is larger than that for a step-index fibre at small V and smaller for large V. The crossover point depends strongly on the value of α. For the particular case of $\alpha = 2$ Petermann [13] has calculated the spot size using the definition given in Equation 24 and there is good agreement with the curve for $\alpha = 2$ in Fig. 5. This is a further justification for the present analysis and for our new definition of spot size for the HE_{11} mode.

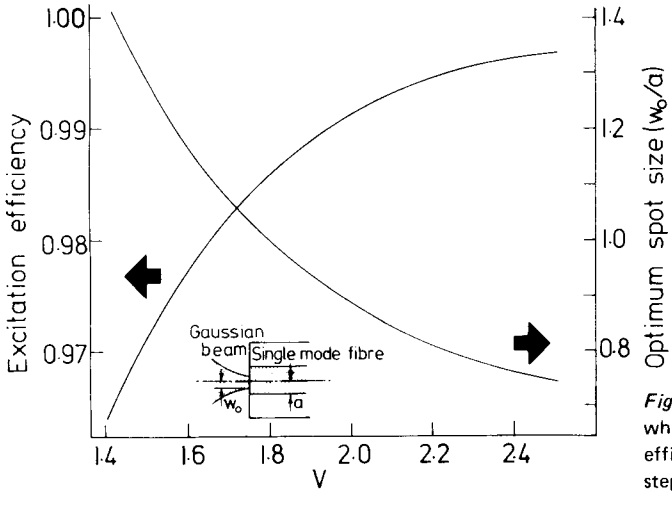

Figure 3 Spot size of the Gaussian beam which gives the maximum excitation efficiency shown when incident on a step-index single-mode fibre.

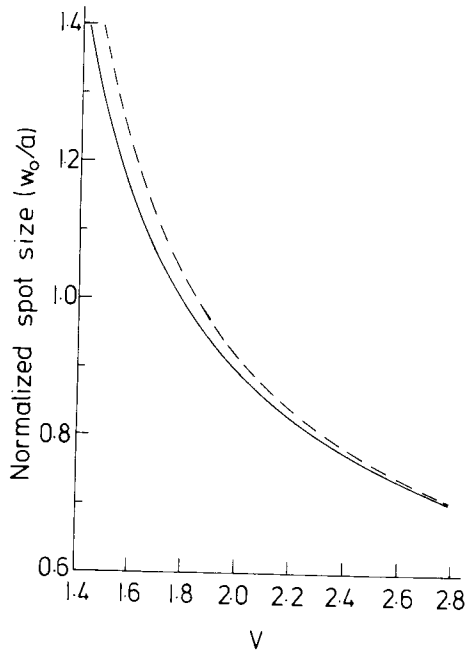

Figure 4 Normalized spot size as a function of normalized frequency for a step-index fibre. The dashed curve is calculated in the usual way from Equation 24 while the solid line corresponds to the proposed new and simplified definition.

The points in Fig. 5 show the limit of single-mode operation (i.e. the cut-off frequencies of the LP_{11} mode) for which the relative spot sizes are 0.78 for the step-index fibre and 0.58 for $\alpha = 2$. Calculations for a specific fibre of $\Delta = 0.002$; $n_2 = 1.459$ and $\lambda = 0.633\,\mu m$ are given in Fig. 6 which shows that the actual spot size depends on V and has a minimum value at a particular value V_m which depends on α. The spot size is a minimum in a step-index fibre and is 10% larger in a fibre having a parabolic refractive-index distribution. One might therefore expect that, for a comparable curvature power spectrum, the microbending loss would also be smaller in a step-index fibre. The dotted line in Fig. 1 indicates that V_m occurs, fortunately, in the single-mode regime and, for each α, at a convenient normalized frequency. Thus the minimum spot size, at least for the example taken, does not change appreciably with α. Furthermore near the minimum the spot size is insensitive to small changes in V.

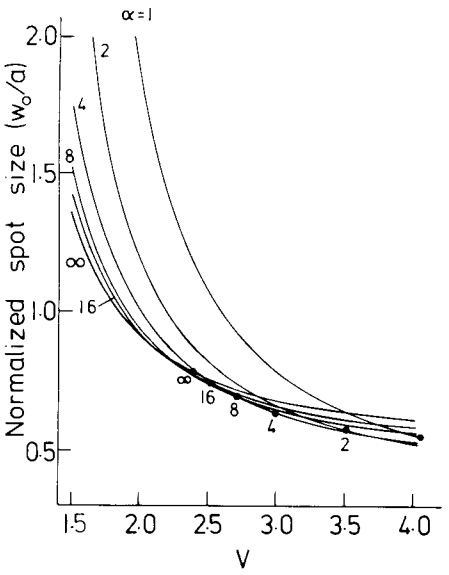

Figure 5 Normalized spot size as a function of normalized frequency for a wide range of refractive-index profiles. The points indicate the cut-off frequency for the value of α indicated.

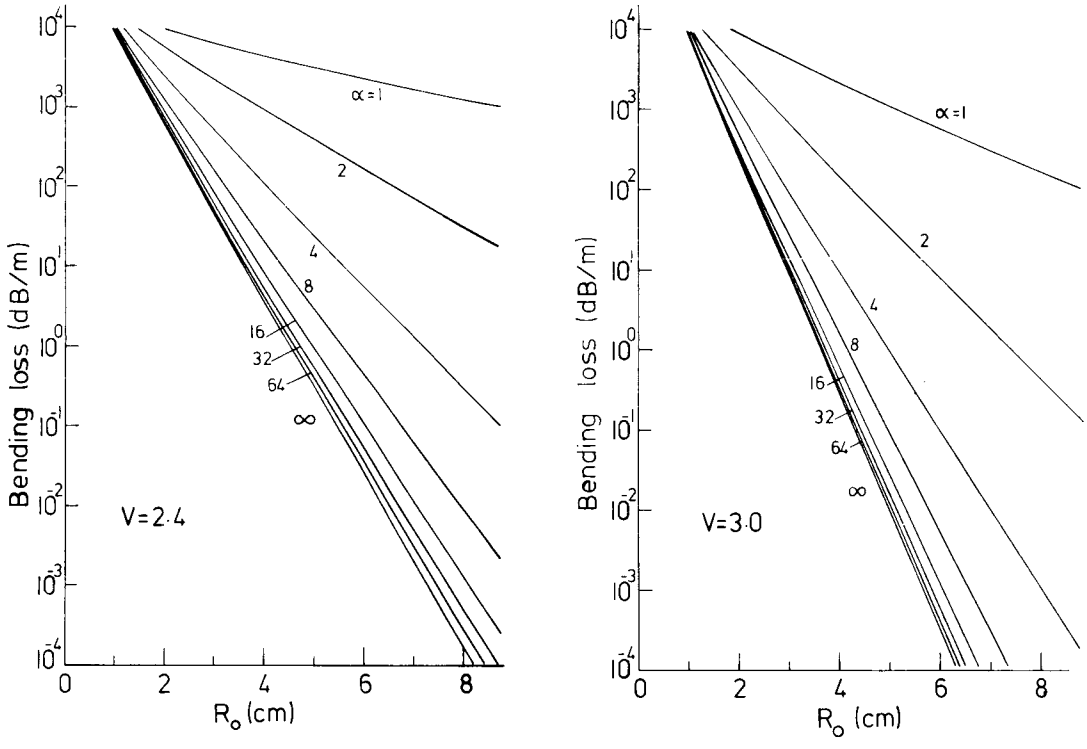

Figure 7 Bending loss as a function of radius of curvature for various profiles at normalized frequencies (a) $V = 2.4$, (b) $V = 3.0$.

The curvature loss indicated is not necessarily typical of those in practical single-mode fibres since it can be reduced appreciably by increasing Δ.

6. Conclusions

The characteristic equation and the field distributions of the HE_{11} mode in a radially inhomogeneous fibre have been obtained under the usual assumption that the index difference between core and cladding is small. The field equations are those of linearly-polarized modes and have been solved by a series expansion method. The convergence of the series is rapid so that the computation time is quite short. Normalized curves of the field distributions and of the mode dispersion for an arbitrary refractive index profile have been deduced. It is found that the cut-off frequency of the LP_{11} mode increases with decreasing α slowly at first but then more rapidly. For example as α falls from ∞ to 10 the cut-off frequency changes by only 5% but increases by 40% as α falls to 2. The spot size, on which the microbending loss is strongly dependent, has been calculated and has its smallest value in a step-index fibre. The spot size in a given fibre is a minimum at a V value which depends on α. For the fibre parameters considered V_m always lies in the single-mode regime and at a convenient normalized frequency. The minimum spot size changes only by 10% from $\alpha = \infty$ to $\alpha = 2$ and thus the corresponding increase in microbending loss is not expected to be large.

For a fixed V number the curvature loss increases rapidly as α is decreased but the change is less marked at the corresponding cut-off frequencies.

References

1. D. GLOGE and E. A. J. MARCATIL, *Bell Syst. Tech. J.* **52** (1973) 1563–78.
2. O. KRUMPHOLZ, *IEE Conference on Trunk Telecommunications by Guided Waves*, IEE Conf. Publ. **71**, (1970) 56–00.
3. W. A. GAMBLING, D. N. PAYNE and H. MATSUMURA, *Elect. Lett.* **13** (1977) 139–40.

4. C. N. KURTZ and W. STREIFER, *IEEE Trans Microwave Theory Tech.* **MTT-17** (1969) 11–15.
5. J. G. DIL and H. BLOK, *Opto. Electronics* **5** (1973) 415–28.
6. T. OKOSHI and K. OKAMOTO, *IEEE Trans Microwave Theory Tech.* **MTT-22** (1974) 938–45.
7. K. OKAMOTO and T. OKOSHI, *ibid* **MTT-24** (1976) 416–21.
8. D. GLOGE, *Appl. Opt.* **10** (1971) 2252–58.
9. K. PETERMANN, *Elect. Lett.* **12** (1976) 107–9.
10. H. MATSUMURA, 'Actual spot size of HE_{11} mode' (ESU Report, August 1976).
11. W. A. GAMBLING, D. N. PAYNE and H. MATSUMURA, *Elect. Lett.* **9** (1973) 412–14.
12. H. MATSUMURA, 'Excitation and coupling efficiencies in a single-mode fibre', (ESU Report, July 1976).
13. K. PETERMANN, *Opt. Quant. Elect.* **9** (1977) 167–75.
14. E. F. KUESTER and D. C. CHANG, *IEEE J. Quant. Elect.* **QE-11** (1975) 903–7.
15. D. MARCUSE, *J. Opt. Soc. Am.* **66** (1976) 311–20.
16. W. A. GAMBLING, D. N. PAYNE and H. MATSUMURA, *Elect. Lett.* **12** (1976) 567–69.
17. W. A. GAMBLING and H. MATSUMURA, *1977 International Conference on Integrated Optics and Optical Communications, Tokyo,* Post-Deadline papers, (1977) 21–4.